Published in final edited form as:
Clin Cancer Res. 2012 December 15; 18(24): 6634–6647. doi:10.1158/1078-0432.CCR-12-1436.

HER2-associated radiation resistance of breast cancer stem cells isolated from HER2-negative breast cancer cells

Nadire Duru[1,*], **Ming Fan**[1], **Demet Candas**[1], **Cheikh Menaa**[1], **Hsin-Chen Liu**[1], **Danupon Nantajit**[1], **Yunfei Wen**[2], **Kai Xiao**[3], **Angela Eldridge**[1,4], **Brett A. Chromy**[4,5], **Shiyong Li**[6], **Douglas R. Spitz**[7], **Kit S. Lam**[3], **Max S. Wicha**[8], and **Jian Jian Li**[1,9,‡]

[1]Department of Radiation Oncology, University of California Davis School of Medicine, Sacramento, CA 95817, USA

[2]Department of Gynecologic Oncology, MD Anderson Cancer Center, University of Texas, Houston, TX 77054, USA

[3]Department of Biochemistry and Molecular Medicine, University of California Davis School of Medicine, Sacramento, CA 95817, USA

[4]Department of Pathology and Laboratory Medicine, University of California Davis School of Medicine, Sacramento, CA 95817, USA

[5]Physical and Life Sciences Directorate, Lawrence Livermore National Laboratory, Livermore, CA 94550, USA

[6]Department of Pathology and Laboratory Medicine, Emory University School of Medicine, Atlanta, GA 30322, USA

[7]Free Radical and Radiation Biology Program, Department of Radiation Oncology, Holden Comprehensive Cancer Center, The University of Iowa, Iowa City, IA52242, USA

[8]University of Michigan Comprehensive Cancer Center, Ann Arbor, MI 48109-5942, USA

[9]NCI-designated Comprehensive Cancer Center, University of California Davis, Sacramento, CA 95817, USA

Abstract

Purpose—To understand the role of HER2-associated signaling network in breast cancer stem cells (BCSCs); using radiation-resistant breast cancer cells and clinical recurrent breast cancers to evaluate HER2-targeted therapy as a tumor eliminating strategy for recurrent $HER2^{-/low}$ breast cancers.

Experimental Design—HER2-expressing BCSCs ($HER2^{+}/CD44^{+}/CD24^{-/low}$) were isolated from radiation-treated breast cancer MCF7 cells and *in vivo* irradiated MCF7 xenograft tumors. Tumor aggressiveness and radiation resistance were analyzed by gap filling, Matrigel invasion, tumor-sphere formation, and clonogenic survival assays. The HER2/CD44 feature was analyzed in 40 primary and recurrent breast cancer specimens. Protein expression profiling in $HER2^{+}/CD44^{+}$/

‡Correspondence: Dr. Jian Jian Li, Department of Radiation Oncology, University of California Davis School of Medicine, 1136 Oak Park Building, 2700 Stockton Boulevard, Sacramento, CA 95817, USA; Phone: 1-916-703-5174; Fax: 1-916-734-4107, jian-jian.li@ucdmc.ucdavis.edu.
*Current Address: California National Primate Research Center, University of California Davis, Davis, CA 95616, USA

AUTHOR CONTRIBUTIONS: N.D., M.F., C.M., and J.J.L. designed research; N.D., M.F., D.C., D.N., Y.W., X.K., A.E., B.A.C., H.L., and S.L. performed research; N.D., D.C., Y.W., B.A.C., D.R.S., K.S.L., M.S.W., and J.J.L. analyzed data; and N.D., D.C., C.M.,D.R.S., M.S.W. and J.J.L. wrote the paper.

CONFLICT OF INTEREST: No potential conflicts of interests were disclosed

$CD24^{-/low}$ versus $HER2^{-}/CD44^{+}/CD24^{-/low}$ BCSCs was conducted with 2-D DIGE and HPLC-MS/MS analysis and HER2-mediated signaling network was generated by MetaCore™ program.

Results—Compared to HER2-negative BCSCs, $HER2^{+}/CD44^{+}/CD24^{-/low}$ cells showed elevated aldehyde dehydrogenase (ALDH) activity and aggressiveness tested by matrigel invasion, tumor sphere formation and *in vivo* tumorigenesis. The enhanced aggressive phenotype and radioresistance of the $HER2^{+}/CD44^{+}/CD24^{-/low}$ cells were markedly reduced by inhibition of HER2 via siRNA or Herceptin treatments. Clinical breast cancer specimens revealed that cells co-expressing HER2 and CD44 were more frequently detected in recurrent (84.6%) than primary tumors (57.1%). In addition, 2-D DIGE and HPLC-MS/MS of $HER2^{+}/CD44^{+}/CD24^{-/low}$ versus $HER2^{-}/CD44^{+}/CD24^{-/low}$ BCSCs reported a unique HER2-associated protein profile including effectors involved in tumor metastasis, apoptosis, mitochondrial function and DNA repair. A specific feature of HER2-STAT3 network was identified.

Conclusion—This study provides the evidence that HER2-mediated pro-survival signaling network is responsible for the aggressive phenotype of breast cancer stem cells that could be targeted to control the therapy-resistant $HER2^{-/low}$ breast cancer.

INTRODUCTION

In spite of advances in early diagnosis and treatment, breast cancer (BC) related death remains significantly high due to resistance of metastatic and recurrent tumors to current anti-cancer regiments; with as many as 40% relapsing with metastatic disease (1, 2). Accumulating evidence of tumor heterogeneity and the presence of CSCs detected in many tumors with the stem cell like characteristics offer new paradigms to understand and generate effective targets to treat recurrent and metastatic tumors (3, 4). BC cells that are able to propagate as mammo-spheres and possess CSC properties are more radioresistant (5) and the population of BCSCs are increased after chemotherapy (6). BC cells surviving radiation show enhanced clonogenic survival indicating the enrichment of radioresistant cells (7, 8).

HER2 belongs to the HER family of transmembrane glycoproteins which consists of four homologous receptors (9). About 25% of BC patients are diagnosed as HER2-amplified status ($HER2^{+}$) associated with a high risk of relapse (10, 11) and targeting HER2 expression inhibits tumor aggressiveness (12, 13). Clinical data show that anti-HER2, Trastuzumab, treatment reduces tumor recurrence when ER+ tumors become resistant to hormonal therapy (14, 15), suggesting that HER2 expression is activated as an escape pro-survival pathway. Consistent with this result, inhibition of HER2 increases tumor cell killing (16, 17). Importantly, overexpression of HER2 is able to increase the CSC population expressing aldehyde dehydrogenase (ALDH) with enhanced invasiveness and tumorigenesis (18). The highest HER2 expression level is detected in tumor-initiating cells of $HER2^{+}$ BC cell lines (19). We have reported that the overexpression of HER2 in $HER2^{-/low}$ MCF7 cells enhances their radioresistance (7) and a NF-κB binding site in the *HER2* promoter region is identified to be responsible for *HER2* transactivation in radiation-treated $HER2^{-/low}$ BC cells (20). However, the exact mechanisms involved in HER2-mediated repopulation of BCSCs under radiation treatment, especially in $HER2^{-/low}$ breast cancer remain to be elucidated.

Here, we identified that HER2-overexpressing BCSCs are responsible for the radioresistance of $HER2^{-/low}$ BC. BCSCs with the feature of $HER2^{+}/CD44^{+}/CD24^{-/low}$, compared to the counterpart $HER2^{-}/CD44^{+}/CD24^{-/low}$ cells, showed an increased aggressiveness, tumorigenesis and radioresistance that can be reduced by siRNA- or Herceptin-mediated HER2 inhibition. Clinical study revealed that HER2 protein expression was enhanced more frequently in the recurrent tumors than primary cancers with an increased rate of co-

expression of HER2 and CD44. Proteomics and connective map studies revealed a unique cluster of HER2-associated effectors including elements in tumor metastasis, redox imbalance, mTOR signaling, and DNA repair. A connective network between HER2 and STAT3 is created. Altogether, our results suggest that HER2-initiated proliferative network is responsible for the resistant phenotype of breast cancer stem cells that are enriched in the therapy-resistant breast cancer.

MATERIALS AND METHODS

Cell culture

Human breast cancer MCF7 cells (ATCC), radiation resistant MCF7/C6 cells (20) and MCF7 cells transfected with HER2, MCF7/HER2 (7) were maintained as described before (20) in Eagle's Minimum Essential Medium (EMEM), supplemented with 10% fetal bovine serum (FBS; HyClone, Logan, UT), 5% sodium pyruvate, 5% non-essential amino acid (NEAA), penicillin (100 units/ml), and streptomycin (100 μg/ml) in a 37 °C incubator (5% CO_2).

Irradiation of xenograft tumor and cells

A standard cell inoculation was used to generate mouse breast cancer xenograft tumors using MCF7 cells as described (20) following the protocol approved by the Institutional Animal Care and Use Committee of University of California Davis (IACUC No. 15315). Eight weeks old female athymic nude mice (Jackson Lab, Bar Harbor, ME) were pretreated for 5 days with estrogen pellets (Innovative Research of America, Sarasota, FL) followed by inoculation with 5×10^6 MCF7 cells. Three weeks after cell inoculation, the average tumor size was 2000 mm^3–2300 mm^3. The mice were divided into two groups; one received sham radiation and the other exposed to local tumor radiation with fractionated doses (5 × 2Gy) delivered by GR-12 irradiator of ^{60}Co γ-rays, under anesthetic agents using ketamine. Twenty hours after the last radiation treatment, mice were sacrificed and tumor cells suspension was prepared for FACS. Radiation was delivered to cultured cells using a Cabinet X-rays System Faxitron Series (dose rate: 0.997 Gy/min; 130 kVp; Hewlett Packard, McMinnville, OR). Cells sheltered from radiation were included as the sham-IR control.

Western blotting

Total cell lysates (20 μg) were separated by SDS-PAGE and blotted onto PVDF membrane. The membrane was incubated with specific primary antibody overnight at 4°C, followed by the horseradish peroxidase-conjugated secondary antibody, and visualized by the ECL Western blotting detection system (Amersham, Arlington Heights, IL). STAT3 antibody was purchased from Santa Cruz (SC-8019). HER2 (MS-730-P) and β-actin antibodies were purchased from Lab Vision Corporation (Fremont, CA) and Sigma (St. Louis, MO), respectively.

Clonogenic survival assay

Standard radiation clonogenic survival assays were performed as previously described (7) following either 0 Gy (sham) or 5 Gy radiation in combination with or without HER2 inhibition by siRNA or Herceptin treatment (10 μg/ml for 5 days with refreshed Herceptin every 48 h). For siRNA treatment, cells were seeded to achieve 30%–50% confluence on the day of transfection and siRNA (20 nM) was transfected using Lipofectamine™ RNAiMAX reagent (Invitrogen, Carlsbad, CA) in antibiotic-free medium for 24 h. Scrambled RNA Duplex (Ambion) and multiple HER2 siRNA were tested and served as negative controls All transfectants were maintained in antibiotic-free complete medium and replaced with

fresh medium before radiation. The colonies were fixed and stained with Coomassie blue and colonies containing more than 50 cells were counted as surviving clones and normalized to the plating efficiency of cells without radiation.

Invasion assay

Aliquots (0.4 ml) of Matrigel (BD biosciences, Sparks, MD) were diluted in serum-free MEM media (Life Technologies, Carlsbad, CA) to the final concentration of 3 mg/ml. Matrigel was then loaded into the upper chamber of 24-well transwell (Costar, Corning, NY) and incubated at 37°C for 1 h before cells (10^5/ml) were added. The lower chamber was filled with 600 μl of MEM media containing 5 μg/ml fibronectin as an adhesive substrate (Santa Cruz biotechnology, San Cruz, CA). The transwell with differently treated cells was incubated for varied times and stained with Diff-Quick Stain (Fisher Scientific; Fairlawn, NJ) and the invasive cells were counted using light microscopy.

Gap filling rate assay

Gap filling capacity was performed as described (21) with 3×10^5 cells grown in each of 6-well plates to 100% confluence followed by culture in medium without serum for 48 h for cell starvation. The gap was created by scraping the cells diagonally with a sterile pipette's tip and the filling capacity was monitored at different times, as specified in results.

Tumor sphere formation

Tumor sphere assay was performed as described (22). Cells were sieved with 40 μm cell strainers (Fisher, Failawn NJ) and single-cell suspensions were seeded into ultra low-attachment 60 mm Petri dishes at a density of 1000 cells/ml. The cells were grown in serum-free mammary epithelial basal medium (MEBM, Lonza, Walkersville, MD), supplemented with B27 (Life Technology, Carlsbad, CA), 20 ng/ml EGF (Biovision, Mountain View, CA), 20 ng/ml basic-FGF, and 4 μg/ml heparin (VWR, Philadelphia PA). Cells were cultured for 10 days and tumor spheres were counted under light microscopy.

Orthotopic mammary fat tumor formation

Tumor initiating test was conducted following the described methods (23, 24) and the protocol was reviewed and approved by the Institutional Animal Care and Use Committee (IACUC) at the University of California Davis (IACUC No. 15315). Eight weeks old female NOD/SCID mice (Jackson Lab, Bar Harbor, ME) were pretreated for 5 days with estrogen pellets (Innovative Research of America, Sarasota FL) and freshly sorted BCSCs were resuspended and diluted in serum-free PBS/Matrigel mixture (1:1 V/V) and inoculated into the mammary pads side by side of the animal using 27G needle (500 cells/injection). Tumorigenesis was assessed twice a week with palpation. Tumor sizes were measured using a caliper and experiments were terminated when tumors reached approximately 1.2 cm in the largest diameter.

Mitochondrial membrane potential (Δψm) and apoptosis

Irradiated cells were incubated with 2 μg/ml of JC-1 for 30 min. The fluorescence intensity of the red precipitate (JC-1 red), and green monomer (JC-1 green) were determined by a plate reader (Spectra Max M^{2e}, Molecular Devices Co., Sunnyvale, CA) at 485nm/595nm or 485nm/525nm (Excitation/Emission). The ratio of JC-1 red (595)/JC-1 green (525) was calculated as $\Delta\Psi m$. For apoptotic analysis, cells were harvested 24 h post-irradiation and were incubated with Annexin-V FITC (Biosource, Carlsbad, CA) and PI (Sigma, St Louis, MO) for 15 min before analysis with FACS-Canto (Becton Dickinson, San Jose, CA).

BCSC sorting

Following described procedures (3), cell suspension was rinsed with PBS with 2% FBS, suspended in PBS containing 0.5% FBS and PI (0.5 mg/ml) and sorted using the Cytopeia inFlux Cell Sorter (BD Biosciences, San Jose, CA). The antibodies applied for sorting were anti-HER2/neu conjugated to allophycocyanin (APC,; BD Biosciences, San Jose, CA), anti-human CD44 conjugated to FITC and human CD24 conjugated to phycoerythrin (PE; Invitrogen, Carlsbad, CA). Cell viability was assessed by 7-AA staining during cell sorting, and by trypan blue exclusion after sorting.

ALDH activity

Cells were suspended (10^6 cells/ml) in ALDEFLUOR assay buffer containing activated ALDH substrate BAAA (BODIPY-aminoacetaldehyde) with or without 50 mM DEAB (diethylaminobenzaldehyde, a specific ALDH inhibitor) and incubated at 37°C for 40 min and analyzed by FACS. The gates were normalized to cells treated with ALDEFLUOR-DEAB.

siRNA-mediated target gene inhibition

The siRNA targeting HER2 was synthesized using the *Silencer* siRNA Construction Kit (Ambion, Austin, TX) with two targeting sequences: 5′ AACCTGGAACTCACCTACCTG 3′ and 5′ AAGCCTCACAGAGATCTTGAA 3′. Cell transfection was performed at 30–50% cell confluence using Lipofectamine_ RNAiMAX reagent (Invitrogen, Carlsbad, CA). Scrambled RNA Duplex (Ambion, Austin, TX) was used for specificity as a negative control.

FISH and IHC of breast cancer specimens

The pathology database was searched for invasive breast cancer, and cases with clinical follow-up were retrieved following Institutional Review Board approval (Emory University IRB#: 901-2004). Total 40 clinical samples were grouped according to pathological classification. Fluorescence *in situ* hybridization (FISH) was performed using the PathVysion kit (Vysis, Inc). A centromere 17:HER2 probe signal ratio of more than 2.2 obtained from 30 interphase nuclei was considered positive for *HER2* gene amplification. Immunohistochemical staining (IHC) was performed using UltraVision LP Detection System HRP Polymer & DAB Plus Chromogen staining kit (Thermo Scientific, Fairlwan, NJ) after heat-induced epitope retrieval. The slides were incubated with anti-HER2 (Sigma, Cat. E2777), anti-CD44 (R&D Systems, Cat. BBA10) and anti-CD24 (Santa Cruz, Cat. Cs-11406) primary antibodies for overnight at 4°C, followed by three washes, and then incubation with the secondary antibodyfor 1 h at RT. The slides were then incubated with DAPI (300 nM in PBS) for 5 min at RT, followed by two washes and then sealed and analyzed with a Nikon microscope (Eclipse, E1000M). Nikon microscope (Eclipse, E1000M) and graded as HER2 + (IHC 2+ and 3+) or amplified (FISH, HER2: centromere 17 signal ratio >2.2); HER2- (IHC 0) or non-amplified (FISH, HER2: centromere 17 signal ratio <1.8); and HER2 equivocal (IHC 1+ and FISH, HER2: centromere 17 signal ratio =1.8 – 2.2).

Two-D DIGE

Total cellular protein (50 μg) was minimally labeled with Cy3 and Cy5 following the reported protocol (25, 26). Labeled samples were mixed together and diluted to 450 μl in rehydration buffer, applied to a 24 cm pH 3–10 NL IPG strips (GE Life Sciences, Fairfield CT) and isoelectric focusing performed until 62500 Vh was reached. The second dimension separation was then performed using 12.5% Tris-Glycine pre-cast gel for 16 h at 2W per gel. CyDye protein spots were imaged on a Typhoon 9410 and differential protein expression

analyzed using DeCyder 6.5 software. Differential In-gel Analysis (DIA) module was used to perform spot detection, quantitation and Cy3/Cy5 volume ratio calculations, fold changes greater than 1.5 were considered significant.

HPLC-MS/MS

For large scale analysis, 1 mg proteins, for each 3 biological replicate samples, were precipitated and processed with SCX (strong cation exchange) column as described (27) followed by a 120 min reverse phase gradient to separate peptides based on their hydrophobicity. The LTQ Orbitrap XL (Thermo Scientific, Waltham, MA) coupled to RP-HPLC system with a low flow ADVANCED Michrom MS source, was set to scan the precursors with a top 4 data-dependent MS/MS method in the profile mode on the precursors and centroid mode on the MS/MS spectra. Tandem mass spectra were analyzed using Mascot database search engine (MatrixScience, London, UK) with mass tolerances set to 1 Da for parent ions and 0.3 Da for MS/MS ions and allowance of up to one missed cleavages. All searches were done against the IPI human database and proteins were considered significant when they met the MASCOT significance threshold of $p > 0.05$.

Gene ontology and protein differential expression assay

The MS and MS/MS data were submitted to Sorcerer Enterprise v.3.5 release (Sage-N Research Inc.) for protein identification against the IPI human protein database. The relative abundance of each identified protein in different samples were analyzed by QTools and Prolucid search algorithm and DTASelect using IP2 (Integrated Proteomics Pipeline) server and Amazon Cloud Computing. Comparative peptide abundance was evaluated by IP2-Census, a Label-free analysis for automated differential peptide/protein spectral counting analysis. Using MetaCore™ Version 6.9, a cluster of proteins and effecters were extracted from the data and identified to interact with both STAT3 and HER2.

Statistical Analysis

The significance of the data was analyzed using an analysis of variance single-factor test and the two-tailed Student *t*-test. A difference was considered significant when $p<0.05$.

RESULTS

Enhanced aggressiveness of radiation-resistant MCF7 cells due to HER2 induction

To identify the key factors responsible for tumor resistance, we first assessed the question of whether HER2 expression is enhanced in the radiation treated $HER2^{-/low}$ breast cancer cells MDA-MB231 cells and a radioresistant cell line (MCF7/C6) that survived a treatment course using fractionated doses of ionizing radiation (8, 20). Consistent with previous observations (7, 20), substantial amount of HER2 proteins was detected in the irradiated MDA-MB231 and the radioresistant cell line MCF7/C6 (Fig. 1A) (20, 28). To further elucidate the mechanism of radiation-induced tumor radioresistance, we studied HER2 expression in MCF7/C6 cell line with MCF7/HER2 and MCF7 wt cells as positive and negative controls, respectively. The induced HER2 protein expression in the MCF7/C6 cells could even reach to the level of HER2 expression in MCF7 cells stably overexpressing HER2 gene (MCF7/HER2). In addition, cell invasiveness of MCF7/C6 cells in Matrigel analysis (Fig. 1B, and Fig. S1C) was also significantly enhanced compared to wt MCF7 cells. Interestingly, the gap-filling capacity remained in a similar rate in all cells except a tendency of increased gap-filling rate of MCF7/C6 and MCF7/HER2 cells at 96 h (Fig. 1B and Fig. S1A). Using tumor sphere formation assay (22) we found that, in addition to increased sizes of tumor spheres, the number of tumor spheres was increased 3.48 and 3.79 folds in MCF7/C6 and MCF7/HER2 cells respectively compared to MCF7 cells (Fig. 1B,

and Fig. S1D). The clonogenicity was increased 2.85 and 2.62 folds in the MCF7/C6 and MCF7/HER2 respectively (Fig. 1B). These results raise the possibility that the expression of *HER2* that was silenced in many HER2$^{-/low}$ breast cancers could be induced in therapy-resistant fraction of cancer cells leading to the overall aggressiveness of recurrent tumors.

HER2^{+}/CD44^{+} cells enriched in irradiated MCF7 cells with increased radiation resistance

Significant reduction in cell sensitivity to IR-induced apoptosis (Fig. 1C) and increased clonogenic survival (Fig. 1C) were detected in HER2 expressing MCF7/C6 and MCF7/HER2 cells compared to wt MCF7 cells. Inhibition of HER2 resulted in reduction of $\Delta\Psi_m$, and HER2 inhibition followed by radiation further reduced $\Delta\Psi_m$ in both MCF7/C6 and MCF7/HER2 cells (Fig. S2). Interestingly, contrary to a similar gap filling rate in all three cell lines without IR (Fig. 1B and Fig. S1A), the gap filling rates were markedly reduced in wt MCF7 cells but remained a relative high level in the MCF7/C6 and MCF7/HER2 cells after radiation (Fig. 1C and Fig. S1B). To verify that the HER2-expressing BCSCs were enriched by multiple IR, we analyzed the expression of HER2 and BCSC markers in irradiated MCF7 cells and xenograft tumors (Fig. 1D; Fig. S3; Table S2). IR was delivered by 5 fractionated doses with 2 Gy each to cells or locally to tumor xenografts in mice. In both cases, CD44^{+}/CD24$^{-/low}$, HER2^{+}/CD44^{+} and HER2^{+}/CD24$^{-/low}$ populations were markedly increased. It should be noticed that about 1% of non-irradiated tumor cells were HER2^{+}/CD44^{+}, but this population was increased about 30-fold after irradiation in xenograft tumors (Fig. 1D, right panel). The HER2^{+}/CD44^{+}/CD24$^{-/low}$ population was also significantly increased (95.8%) in the radio-resistant MDA-MB231 cells (Fig. S4; The FIR Clone 4 was derived from the triple negative wild type MDA-MB231 cells after long-term irradiation, 20). Similar to MCF7/C6, the increase in the HER2^{+}/CD44^{+}/CD24$^{-/low}$ subpopulation was due to the induction of HER2 expression in response to irradiation. However, the CD44^{+}/CD24^{-} cells *per se* did not significantly change compared to the wt cells, probably due to the fact that MDA-MB-231 cells were found to hold naturally a high level of BCSCs (29, 30). The high level of BCSCs may explain the inherited aggressiveness phenotype of MDA-MB-231 compared to MCF7 cells. However, we believe that the overexpression of HER2 will further increase their aggressiveness and resistance to radiation.

Furthermore, we found that the increased population of HER2^{+}/CD44^{+} cells was further enhanced in the irradiated xenograft tumors (Fig. 1D right panel) compared to irradiated cells in culture (Fig. 1D, left panel), highlighting the possible role of other factors in the development of radioresistant BCSCs in vivo Taken together, these data suggest that the tumor microenvironment under therapeutic stress conditions promotes the survival of HER2-expressing BCSCs. These results reinforce our hypothesis that HER2 expression in BCSC is a predominant feature of radiation resistance in HER2$^{-/low}$ cancer.

Identification of HER2^{+}/CD44^{+}/CD24$^{-/low}$ cells

To investigate whether HER2 expression is a unique marker of radioresistant BCSCs in HER2$^{-/low}$ BC cells, CD44^{+}/CD24$^{-/low}$ population was further sorted according to the level of HER2 expression (Fig. 2A, B and Table S1). Of the total of 2.4×10^6 MCF7/C6 cells, 3.7×10^4 cells were identified as CD44^{+}/CD24$^{-/low}$ (1.51%). Interestingly, only 9.84% of the CD44^{+}/CD24$^{-/low}$ population was detected to express a high level of HER2 (termed as HER2^{+}/CD44^{+}/CD24$^{-/low}$ population) and 6.85% showed low expression (termed as HER2^{-}/CD44^{+}/CD24$^{-/low}$ population; Fig. 2B and Table S1). The difference in HER2 expression between these two populations was confirmed by immunoblotting (Fig. 2B, right panel). ALDH is established to play a major role in cell death resistance and is associated with BCSCs' aggressiveness (31). We found that the ALDH activity was about 3-fold elevated in HER2^{+}/CD44^{+}/CD24$^{-/low}$ cells compared to their counterpart HER2^{-}/CD44^{+}/

$CD24^{-/low}$ population (Fig. 2C and D).. These results provide the evidence indicating that a fraction of HER2-expressing $CD44^{+}/CD24^{-/low}$ BCSCs is present in the surviving BC cells with status of $HER2^{-/low}$.

Enhanced aggressiveness of $HER2^{+}/CD44^{+}/CD24^{-/low}$ BCSCs

The $HER2^{+}/CD44^{+}/CD24^{-/low}$ BCSCs were more aggressive in migration compared to the $HER2^{-}/CD44^{+}/CD24^{-/low}$ BCSCs under the condition of sham or 5 Gy IR (Fig. 3C, and Fig S4), indicating that HER2-expressing BCSCs are more resistant to genotoxic stress. The increased radioresistance of $HER2^{+}/CD44^{+}/CD24^{-/low}$ BCSCs was further supported by elevated $\Delta\Psi_m$, reduced apoptosis, and increased clonogenic survival (Fig. 3A, B). In addition, the invasiveness and tumor sphere formation (Fig. 3C) were increased ~5 and ~4 fold respectively in $HER2^{+}/CD44^{+}/CD24^{-/low}$ cells compared to the $HER2^{-}/CD44^{+}/CD24^{-/low}$ cells. To elucidate whether HER2 expression endows BCSC a higher tumorigenic capacity, we measured tumor formation of $HER2^{+}/CD44^{+}/CD24^{-/low}$ versus $HER2^{-}/CD44^{+}/CD24^{-/low}$ cells using NSG/SCID mouse xenograft model. HER2 status, indeed, affects the tumor-initiating rate of BCSCs. All the sites inoculated with $HER2^{+}/CD44^{+}/CD24^{-/low}$ cells (500 cells/injection, $HER2^{+}$) developed tumors (6/6) with an average volume of 92 mm^3 at day 21; whereas no detectable tumors were recorded in all sites (0/6) with the same number of $HER2^{-}/CD44^{+}/CD24^{-/low}$ cells ($HER2^{-}$) up to day 45 (Fig. 3C). To verify the direct function of HER2 expression in radioresistance, siRNA-mediated HER2 inhibition was applied and the results showed a reduction in cell invasiveness by ~70% that was further reduced by HER2 inhibition combined with 5 Gy IR (Fig. 4A). Noticeably, the gap filling rates were also severely reduced by HER2 inhibition with or without combination with IR (Fig. 4B, Fig. S5). In agreement, treatment with HER2 siRNA (Fig. 4C) or Herceptin (Fig. 4D) reduced the clonogenicity of $HER2^{+}/CD44^{+}/CD24^{-/low}$ BCSCs, which was further decreased when combined with IR treatment.

Co-expression of HER2 and CD44 in recurrent breast cancer

To investigate whether the feature of $HER2^{+}/CD44^{+}/CD24^{-/low}$ is related to the aggressiveness of metastatic breast cancers, we analyzed the expression of HER2, CD44, and CD24 in 40 randomly-selected pathological specimens that are clinically diagnosed as primary, recurrent or unknown breast tumors by the pathology department at the Emory University School of Medicine. In each tumor, we correlated the degree of HER2 gene amplification assessed by FISH (fluorescent in situ hybridization,) with the HER2 protein expression detected by IHC (immunohistochemistry). By FISH analysis, 12 of 40 tumors were determined as HER2 amplified (30%), whereas HER2 protein was expressed in 33 of 40 tumors by IHC (82.5%; Fig. 5A), suggesting that mechanisms other than gene amplification are responsible for the enhanced expression of HER2 protein. Interestingly, cells positively stained with HER2 and CD44 antibody by IHC were significantly increased (11/13, 85%) in the recurrent tumor samples compared to the level of the samples of primary tumors (12/21, 57%; Fig. 5B). Subsequently, 85% of the recurrent tumors were $CD24^{-}$ contrasted with 48% in primary tumors (Fig. S6C). A representative picture of the tumors co-stained with HER2 and CD44 without CD24 expression are shown in Fig. S6D. Taken together, these results support that HER2 expressing BCSC are enriched in recurrent breast tumors.

Proteomics of $HER2^{+}/CD44^{+}/CD24^{-/low}$ versus $HER2^{-}/CD44^{+}/CD24^{-/low}$ cells

To identify the signaling network causing the aggressive growth of HER2-expressing BCSCs, we conducted proteomics experiments using 2-D DIGE (Fig. S7) and reverse-phase high-performance LC/MS/MS (Fig. S7, Tables S3 and S4) that revealed a specific protein profile differentially regulated in $HER2^{+}/CD44^{+}/CD24^{-/low}$ compared to the $HER2^{-}/CD44^{+}/CD24^{-/low}$ BCSCs. 2-D DIGE results highlighted differences between these two

samples and additional proteomics using reverse-phase high-performance LC/MS/MS to separate trypsin-digested peptides identified 6537 peptides differentially expressed in $HER2^{+}/CD44^{+}/CD24^{-/low}$ versus $HER2^{-}/CD44^{+}/CD24^{-/low}$ cells. Using peptide counts determining differential proteins, 499 and 182 proteins were up-regulated respectively in $HER2^{+}/CD44^{+}/CD24^{-/low}$ and $HER2^{-}/CD44^{+}/CD24^{-/low}$ cells (cutoff fold change ≥ 2). These peptides and proteins were further grouped according to their cellular functions and a representative list was presented according to functions of tumor metastasis, mTOR signaling, apoptosis, mitochondrial function, redox balancing (Table S3).

Cross-talk between HER2 and STAT3 in $HER2^{+}/CD44^{+}/CD24^{-/low}$ BCSCs

Among the key signaling elements and effectors involved in tumor proliferation and metastasis found in our protein expression profiling (Table S3), the expressions of STAT3 and Src were detected in $HER2^{+}/CD44^{+}/CD24^{-/low}$ but not in the $HER2^{-}/CD44^{+}/CD24^{-/low}$ BCSCs (Table S3). Since HER2 is known to activate STAT3 through both JAK2- and Src-dependent manners (32), resulting in tumor aggressiveness, we confirmed the co-expression of HER2 and STAT3 in $HER2^{+}/CD44^{+}/CD24^{-/low}$ but not in $HER2^{-}/CD44^{+}/CD24^{-/low}$ BCSCs by Western blotting (Fig. 6A), and immunofluorescence and immunohistochemical analyses (Fig. 6C and D). Reporter gene analysis showed increased activity of STAT3 promoter only in HER2 expressing BCSCs (Fig. 6B). As shown in Fig 6D, the overexpression of HER2 (green membrane) in radio-resistant cancer cells is strongly associated with high levels of STAT3 (red cytoplasmic); and STAT3 level is low in cells that are not expressing HER2 protein. Interestingly $HER2^{+}$ positive human specimen showed similar pattern of co-expression of HER2 and STAT3. Taken together these data suggest a possible strong connection between HER2 and STAT3 signaling pathways. Furthermore, using the MetaCore™ Version 6.9 program, we created the HER2-STAT3 signaling network consisting of all effectors that are directly linked to both HER2 and STAT3. This network revealed c-Src kinase that was expressed in $HER2^{-}/CD44^{+}/CD24^{-/low}$ BCSCs (Table S3) as one of the mediators in the HER2-STAT3 connection (Fig. 6E). Interestingly, recently Korkaya *et al.* reported that STAT3 activation might account for Herceptin resistance in HER^{+} breast cancer cells due to the expression and secretion of IL-6 (33). Thus, IL6 could be one of the factors mediating the radio-resistance of cancer stem cells in $HER^{-/low}$ breast cancers. Further investigation of the HER2-STAT3 signaling network and other HER2-linked effectors and pathways may generate additional mechanistic insights to understand the aggressive phenotype of cancer stem cells.

Discussion

Increasing evidence supports the concept that the tumor bulk is consisted of heterogeneous population and potentially contains tumor-initiating cells or cancer stem cells (34, 35). Here we identified HER2-expressing $CD44^{+}/CD24^{-/low}$ BCSCs from both *in vivo* and *in vitro* irradiated $HER2^{-/low}$ BC cells and tumor samples from breast cancer patients. Compared to the HER2-negative BCSCs, $HER2^{+}/CD44^{+}/CD24^{-/low}$ cells showed a more aggressive phenotype and *in vivo* tumorigenesis with the enhanced resistance to radiation. Cells co-expressing HER2 and CD44 were more frequently detected in recurrent than the primary tumors in breast cancer patients. Our results further provide a unique group of proteins in $HER2^{+}/CD44^{+}/CD24^{-/low}$ cells governing therapy outcomes including metastasis, mTOR signaling, apoptosis, mitochondrial function, redox balancing, DNA repair and HER2-STAT3 prosurvival network. These results suggest that HER2-expressing BCSCs may be effective targets to treat recurrent tumors.

Although CSCs isolated from many tumors show an increased tumor-initiating ability and invasiveness, not all CSCs are able to reside and proliferate at sites of metastasis (36). These results raise an important question regarding whether or not CSCs are themselves a

heterogenic population. Using patient-derived xenograft tumors, different radiation sensitivities were detected in the CSC population (37), supporting that not all BCSCs are radioresistant. HER2-positive breast cancer are resistant to an array of therapies with a high risk of local relapse and recurrence (38) and blocking HER2 expression or using specific agents targeting HER2 signaling pathway (Trastuzumab, Lapatinib, and others) improve the cancer control (16). However, this benefit is not only reported for the $HER2^{+}$ tumors, but also for patients with $HER2^{-/low}$ status (39, 40), suggesting that acquired resistance due to HER2 induction could develop under anti-cancer treatments. In fact, we have demonstrated that HER2 expression is inducible in $HER2^{-/low}$ BC cells via NFκB-mediated HER2 promoter transactivation and the induced HER2 activation is responsible for the resistance to radiation (20). Our present data suggest that HER2-expressing BCSCs grow more aggressively than HER2-negative BCSCs under genotoxic conditions. Thus, tumor cells surviving a course of anti-cancer radiotherapy are likely enriched with more aggressive cancer cells expressing HER2.

A dynamic repopulation process may be initiated in tumors under chemo- and/or radiotherapy (5, 41, 42). In agreement with reported BCSC resistant phenotype, BCSCs were increased in the surviving fraction of $HER2^{-/low}$ MCF7 cells and xenograft tumors after exposure to multiple doses of irradiation (Fig. 1D). Together with an increased frequency of $HER2^{+}/CD44^{+}$ in the recurrent tumors (Fig. 5A and B), these results raised the possibility that breast tumors originally diagnosed as $HER2^{-/low}$ status (mainly by *HER2* transcript enhancements), may be induced to express a high level of HER2 protein. Thus, the radioresistant fraction within the $CD44^{+}/CD24^{-/low}$ population could be enriched due to HER2 expression, an oncogene well-recognized in tumor resistance, metastasis, and tumor relapse (10, 11, 43). In this regard, HER2 protein expression could be more enhanced while *HER2* gene copies may remain constant. These results may explain the additional curative benefit gained with Trastuzumab as a co-adjuvant for patients initially classified as $HER2^{-}$ candidates (39, 40). It is highly possible that genotoxic agents that activate NFκB, may result in a selection of BCSCs with the feature of $HER2^{+}/CD44^{+}/CD24^{-/low}$ in the $HER2^{-/low}$ breast cancer.

In agreement with the low population of cancer stem cells (44), we found that 1.5–2.0% of the radioresistant MCF7/C6 cells contain the feature of $CD44^{+}/CD24^{-/low}$ in which, 9.8% was detected as $HER2^{+}/CD44^{+}/CD24^{-/low}$ cells (Fig. 2). The $HER2^{+}/CD44^{+}/CD24^{-/low}$ BCSCs showed 4–5 folds increase in cell invasion, tumor sphere formation with an enhanced *in vivo* tumorigenesis (Fig. 3C). Although the tumor-initiating capacity of $CD44^{+}/CD24^{-/low}$ cells isolated from both primary patient tumors and immortalized cell lines is well established, our data suggested that $CD44^{+}/CD24^{-/low}$ cells fail to grow tumors when HER2 is not expressed ($HER2^{+}/CD44^{+}/CD24^{-/low}$ versus $HER2^{-}/CD44^{+}/CD24^{-/low}$ cells, Fig. 3C) (18). Importantly, tumors with HER2 protein expression were obviously increased in the recurrent breast cancer tissues than the primary lesions, and the feature of $HER2^{+}/CD44^{+}/CD24^{-/low}$ was more frequently detected in recurrent tumors compared to the primary tumors (Fig. 5). Therefore, it is highly possible that a small fraction of BCSCs with elevated *de novo* HER2 expression in $HER2^{-/low}$ BC has the survival advantage under genotoxic condition such as ionizing radiation or anti-cancer chemotherapy and thus will allow repopulation after a course of treatment. However, we could not exclude the possibility that *HER2* transactivation is preferably induced in a specific fraction of BCSC population under genotoxic stress that is responsible for tumor repopulation.

It has been reported that CD44 and HER2 interaction promotes human ovarian tumor (45). Clinically, although $CD44^{+}/CD24^{-/low}$ BCSC phenotype has been linked to basal-type BC tumors, particularly in BRCA1 inherited cancers, this phenotype does not correlate with the clinical outcome (46), suggesting that, besides the feature of $CD44^{+}/CD24^{-/low}$, specific

pro-survival networks are associated with CSC resistance. ALDH, a key BCSC marker, also present in only about 30% of tumors, further divide the $CD44^+/CD24^{-/low}$ population into highly tumorigenic $ALDH^+/CD44^+/CD24^{-/low}$ that is capable of generating tumors as low as 20 cells; whereas $ALDH^-/CD44^+/CD24^{-/low}$ show reduced tumorigenesis (31). Unlike $CD44^+/CD24^{-/low}$, the ALDH phenotype correlates with clinical outcome, tumor grade, and the status of HER2 and Ki67. Korkaya *et al* reported that HER2 overexpression enhances the ALDH activity (18) and Diehn *et al* found that $ALDH^+$/HER2 cells are more tumorigenic than $ALDH^-$ cells (6), further confirming the link between ALDH activity, HER2 expression and CSCs. In this study, we found that ALDH activity is elevated in the HER2-expresing $CD44^+/CD24^{-/low}$ cells (Fig. 2C and D), suggesting that this radioresistant subpopulation of BCSCs is able to activate both HER2 and ALDH. Thus, $ALDH^+/HER^+$ and their potential downstream effectors may provide more specific sets of targets to treat metastatic and recurrent BC, which needs to be further investigated.

To identify key factors causing the resistant phenotype of $HER2^+/CD44^+/CD24^{-/low}$ cells, our proteomics data from LC/MS/MS revealed a comprehensive protein profile in $HER2^+/CD44^+/CD24^{-/low}$ versus $HER2^-/CD44^+/CD24^{-/low}$ BCSCs (Table S3). The strong pro-survival and anti-apoptotic factors are believed to be the major mechanism the resistance of CSCs to radiation and chemotherapy (47, 48). Although many of these proteins are already known for cell survival such as DNA repair (Table S3) (47) (49), angiogenesis (41), cell adhesion and proliferation (50), elements involved in metastasis, mTOR signaling, mitochondrial ATP generation and redox balancing seem to be required for the enhanced aggressiveness in HER2-expressing BCSCs. A lowered rate of apoptosis in CSCs (50) with enhanced mitochondrial function and DNA repair ability contributes to the BCSC survival. Among key proteins and effectors detected in the in the $HER2^+/CD44^+/CD24^{-/low}$ versus $HER2^-/CD44^+/CD24^{-/low}$ BCSCs profile, we found that STAT3 was expressed in $HER2^+/CD44^+/CD24^{-/low}$ but not in $HER2^-/CD44^+/CD24^{-/low}$ BCSCs (Table S3). Since HER2 is known to activate STAT3 through both JAK2- and Src-dependent manners (32) and STAT3 promotes the microRNA expression and chemoresistance in CD44-activated head and neck cancer cells (51), our data on the co-activation of HER2 and STAT3 further illustrate a HER2-STAT3 signaling network related to the aggressiveness of HER2-expressing BCSCs (Fig. 6D). Further investigation of the HER2-STAT3 network and other HER2-linked pathways may generate additional mechanistic insights to understand the development of aggressive cancer stem cells.

In summary, these results have important implications as they suggest that HER2-overexpressing breast cancer stem cells are causally associated with the aggressive phenotype and radioresistance of $HER2^{-/low}$ breast cancer cells. The ability of $HER2^+/CD44^+/CD24^{-/low}$ to display an enhanced aggressiveness suggests that the co-expression of HER2 and CD44 is a unique feature of BCSCs in $HER2^{-/low}$ breast cancer. The HER2-associated prosurvival signaling network including the STAT3 pathway could be enhanced due to a substantial HER2 gene transactivation during or after anti-cancer therapy. Therefore, further characterization of HER2-initiated pathways in the therapy-resistant cancer stem cells, especially the HER2-STAT3 crosstalk (Fig. 6E) identified in this study, may generate new targets for the control of recurrent and metastatic tumors.

Supplementary Material

Refer to Web version on PubMed Central for supplementary material.

Acknowledgments

We thank Dr. Terry D. Oberley at the University of Wisconsin-Madison, Dr. William C. Dewey at the University of California San Francisco, and members of our laboratory for valuable suggestions and discussions; Khatereh Motamedchaboki at the Proteomics Facility at Sanford-Burnham Medical Research Institute for assistance in mass spectrometry analysis.

GRANT SUPPORT: This work was supported by National Institutes of Health Grant CA133402, CA152313 (JJL) and CA133114 (DRS) as well as the Department of Energy Office of Science Grant DE-SC0001271 (JJL).

References

1. Dowsett M, Harper-Wynne C, Boeddinghaus I, Salter J, Hills M, Dixon M, et al. HER-2 amplification impedes the antiproliferative effects of hormone therapy in estrogen receptor-positive primary breast cancer. Cancer Res. 2001; 61:8452–8. [PubMed: 11731427]
2. Massarweh S, Osborne CK, Jiang S, Wakeling AE, Rimawi M, Mohsin SK, et al. Mechanisms of tumor regression and resistance to estrogen deprivation and fulvestrant in a model of estrogen receptor-positive, HER-2/neu-positive breast cancer. Cancer Res. 2006; 66:8266–73. [PubMed: 16912207]
3. Al-Hajj M, Wicha MS, Benito-Hernandez A, Morrison SJ, Clarke MF. Prospective identification of tumorigenic breast cancer cells. Proc Natl Acad Sci U S A. 2003; 100:3983–8. [PubMed: 12629218]
4. Wicha MS. Targeting breast cancer stem cells. Breast. 2009; 18 (Suppl 3):S56–8. [PubMed: 19914544]
5. Phillips TM, McBride WH, Pajonk F. The response of CD24(−/low)/CD44+ breast cancer-initiating cells to radiation. J Natl Cancer Inst. 2006; 98:1777–85. [PubMed: 17179479]
6. Diehn M, Cho RW, Lobo NA, Kalisky T, Dorie MJ, Kulp AN, et al. Association of reactive oxygen species levels and radioresistance in cancer stem cells. Nature. 2009; 458:780–3. [PubMed: 19194462]
7. Guo G, Wang T, Gao Q, Tamae D, Wong P, Chen T, et al. Expression of ErbB2 enhances radiation-induced NF-kappaB activation. Oncogene. 2004; 23:535–45. [PubMed: 14724581]
8. Li Z, Xia L, Lee ML, Khaletskiy A, Wang J, Wong JYC, et al. Effector genes altered in MCF-7 human breast cancer cells after exposure to fractionated ionizing radiation. Radiat Res. 2001; 155:543–53. [PubMed: 11260656]
9. Olayioye MA. Update on HER-2 as a target for cancer therapy: intracellular signaling pathways of ErbB2/HER-2 and family members. Breast Cancer Res. 2001; 3:385–9. [PubMed: 11737890]
10. Haffty BG, Brown F, Carter D, Flynn S. Evaluation of HER-2 neu oncoprotein expression as a prognostic indicator of local recurrence in conservatively treated breast cancer: a case-control study. Int J Radiat Oncol Biol Phys. 1996; 35:751–7. [PubMed: 8690641]
11. Holbro T, Beerli RR, Maurer F, Koziczak M, Barbas CF 3rd, Hynes NE. The ErbB2/ErbB3 heterodimer functions as an oncogenic unit: ErbB2 requires ErbB3 to drive breast tumor cell proliferation. Proc Natl Acad Sci U S A. 2003; 100:8933–8. [PubMed: 12853564]
12. Wang SC, Zhang L, Hortobagyi GN, Hung MC. Targeting HER2: recent developments and future directions for breast cancer patients. Semin Oncol. 2001; 28:21–9. [PubMed: 11774202]
13. Li YM, Pan Y, Wei Y, Cheng X, Zhou BP, Tan M, et al. Upregulation of CXCR4 is essential for HER2-mediated tumor metastasis. Cancer Cell. 2004; 6:459–69. [PubMed: 15542430]
14. Arpino G, Wiechmann L, Osborne CK, Schiff R. Crosstalk between the estrogen receptor and the HER tyrosine kinase receptor family: molecular mechanism and clinical implications for endocrine therapy resistance. Endocr Rev. 2008; 29:217–33. [PubMed: 18216219]
15. Massarweh S, Osborne CK, Creighton CJ, Qin L, Tsimelzon A, Huang S, et al. Tamoxifen resistance in breast tumors is driven by growth factor receptor signaling with repression of classic estrogen receptor genomic function. Cancer Res. 2008; 68:826–33. [PubMed: 18245484]
16. Jones KL, Buzdar AU. Evolving novel anti-HER2 strategies. Lancet Oncol. 2009; 10:1179–87. [PubMed: 19959074]

17. Kurokawa H, Arteaga CL. Inhibition of erbB receptor (HER) tyrosine kinases as a strategy to abrogate antiestrogen resistance in human breast cancer. Clin Cancer Res. 2001; 7:4436s–42s. discussion 11s–12s. [PubMed: 11916237]
18. Korkaya H, Paulson A, Iovino F, Wicha MS. HER2 regulates the mammary stem/progenitor cell population driving tumorigenesis and invasion. Oncogene. 2008; 27:6120–30. [PubMed: 18591932]
19. Magnifico A, Albano L, Campaner S, Delia D, Castiglioni F, Gasparini P, et al. Tumor-initiating cells of HER2-positive carcinoma cell lines express the highest oncoprotein levels and are sensitive to trastuzumab. Clin Cancer Res. 2009; 15:2010–21. [PubMed: 19276287]
20. Cao N, Li S, Wang Z, Ahmed KM, Degnan ME, Fan M, et al. NF-kappaB-mediated HER2 overexpression in radiation-adaptive resistance. Radiat Res. 2009; 171:9–21. [PubMed: 19138055]
21. Song G, Zhang Y, Wang L. MicroRNA-206 targets notch3, activates apoptosis, and inhibits tumor cell migration and focus formation. J Biol Chem. 2009; 284:31921–7. [PubMed: 19723635]
22. Dontu G, Abdallah WM, Foley JM, Jackson KW, Clarke MF, Kawamura MJ, et al. In vitro propagation and transcriptional profiling of human mammary stem/progenitor cells. Genes Dev. 2003; 17:1253–70. [PubMed: 12756227]
23. Al-Hajj M, Clarke MF. Self-renewal and solid tumor stem cells. Oncogene. 2004; 23:7274–82. [PubMed: 15378087]
24. Clarke MF. A self-renewal assay for cancer stem cells. Cancer Chemother Pharmacol. 2005; 56 (Suppl 1):64–8. [PubMed: 16273355]
25. Corzett TH, Fodor IK, Choi MW, Walsworth VL, Turteltaub KW, McCutchen-Maloney SL, et al. Statistical analysis of variation in the human plasma proteome. J Biomed Biotechnol. 2010; 2010:258494. [PubMed: 20130815]
26. Corzett TH, Fodor IK, Choi MW, Walsworth VL, Chromy BA, Turteltaub KW, et al. Statistical analysis of the experimental variation in the proteomic characterization of human plasma by two-dimensional difference gel electrophoresis. J Proteome Res. 2006; 5:2611–9. [PubMed: 17022632]
27. Brill LM, Motamedchaboki K, Wu S, Wolf DA. Comprehensive proteomic analysis of Schizosaccharomyces pombe by two-dimensional HPLC-tandem mass spectrometry. Methods. 2009; 48:311–9. [PubMed: 19272449]
28. Guo G, Yan-Sanders Y, Lyn-Cook BD, Wang T, Tamae D, Ogi J, et al. Manganese superoxide dismutase-mediated gene expression in radiation-induced adaptive responses. Mol Cell Biol. 2003; 23:2362–78. [PubMed: 12640121]
29. Jo M, Lester RD, Montel V, Eastman B, Takimoto S, Gonias SL. Reversibility of epithelial-mesenchymal transition (EMT) induced in breast cancer cells by activation of urokinase receptor-dependent cell signaling. J Biol Chem. 2009; 284:22825–33. [PubMed: 19546228]
30. Yin H, Glass J. The phenotypic radiation resistance of CD44+/CD24(−or low) breast cancer cells is mediated through the enhanced activation of ATM signaling. PLoS ONE. 2011; 6:e24080. [PubMed: 21935375]
31. Ginestier C, Hur MH, Charafe-Jauffret E, Monville F, Dutcher J, Brown M, et al. ALDH1 is a marker of normal and malignant human mammary stem cells and a predictor of poor clinical outcome. Cell Stem Cell. 2007; 1:555–67. [PubMed: 18371393]
32. Ren Z, Schaefer TS. ErbB-2 activates Stat3 alpha in a Src- and JAK2-dependent manner. J Biol Chem. 2002; 277:38486–93. [PubMed: 11940572]
33. Korkaya H, Kim GI, Davis A, Malik F, Henry NL, Ithimakin S, et al. Activation of an IL6 inflammatory loop mediates trastuzumab resistance in HER2+ breast cancer by expanding the cancer stem cell population. Mol Cell. 2012
34. Al-Ejeh F, Smart CE, Morrison BJ, Chenevix-Trench G, Lopez JA, Lakhani SR, et al. Breast cancer stem cells: treatment resistance and therapeutic opportunities. Carcinogenesis. 2011; 32:650–8. [PubMed: 21310941]
35. Croker AK, Allan AL. Inhibition of aldehyde dehydrogenase (ALDH) activity reduces chemotherapy and radiation resistance of stem-like ALDH(hi)CD44 (+) human breast cancer cells. Breast Cancer Res Treat. 201110.1007/s10549-011-1692-y

36. Sheridan C, Kishimoto H, Fuchs RK, Mehrotra S, Bhat-Nakshatri P, Turner CH, et al. CD44+/CD24− breast cancer cells exhibit enhanced invasive properties: an early step necessary for metastasis. Breast Cancer Res. 2006; 8:R59. [PubMed: 17062128]
37. Zielske SP, Spalding AC, Wicha MS, Lawrence TS. Ablation of breast cancer stem cells with radiation. Transl Oncol. 2011; 4:227–33. [PubMed: 21804918]
38. Gonzalez-Angulo AM, Stemke-Hale K, Palla SL, Carey M, Agarwal R, Meric-Berstam F, et al. Androgen receptor levels and association with PIK3CA mutations and prognosis in breast cancer. Clin Cancer Res. 2009; 15:2472–8. [PubMed: 19276248]
39. Perez EA, Reinholz MM, Hillman DW, Tenner KS, Schroeder MJ, Davidson NE, et al. HER2 and chromosome 17 effect on patient outcome in the N9831 adjuvant trastuzumab trial. J Clin Oncol. 2010; 28:4307–15. [PubMed: 20697084]
40. Ardavanis A, Kountourakis P, Kyriakou F, Malliou S, Mantzaris I, Garoufali A, et al. Trastuzumab plus paclitaxel or docetaxel in HER-2-negative/HER-2 ECD-positive anthracycline- and taxane-refractory advanced breast cancer. Oncologist. 2008; 13:361–9. [PubMed: 18448549]
41. Bao S, Wu Q, McLendon RE, Hao Y, Shi Q, Hjelmeland AB, et al. Glioma stem cells promote radioresistance by preferential activation of the DNA damage response. Nature. 2006; 444:756–60. [PubMed: 17051156]
42. Dalerba P, Cho RW, Clarke MF. Cancer stem cells: models and concepts. Annu Rev Med. 2007; 58:267–84. [PubMed: 17002552]
43. Slamon DJ. Studies of the HER-2/neu proto-oncogene in human breast cancer. Cancer Invest. 1990; 8:253. [PubMed: 1976032]
44. Al-Hajj M, Becker MW, Wicha M, Weissman I, Clarke MF. Therapeutic implications of cancer stem cells. Curr Opin Genet Dev. 2004; 14:43–7. [PubMed: 15108804]
45. Bourguignon LY, Zhu H, Chu A, Iida N, Zhang L, Hung MC. Interaction between the adhesion receptor, CD44, and the oncogene product, p185HER2, promotes human ovarian tumor cell activation. J Biol Chem. 1997; 272:27913–8. [PubMed: 9346940]
46. Honeth G, Bendahl PO, Ringner M, Saal LH, Gruvberger-Saal SK, Lovgren K, et al. The CD44+/CD24− phenotype is enriched in basal-like breast tumors. Breast Cancer Res. 2008; 10:R53. [PubMed: 18559090]
47. Ropolo M, Daga A, Griffero F, Foresta M, Casartelli G, Zunino A, et al. Comparative analysis of DNA repair in stem and nonstem glioma cell cultures. Mol Cancer Res. 2009; 7:383–92. [PubMed: 19276180]
48. Johannessen TC, Bjerkvig R, Tysnes BB. DNA repair and cancer stem-like cells--potential partners in glioma drug resistance? Cancer Treat Rev. 2008; 34:558–67. [PubMed: 18501520]
49. Frosina G. DNA repair in normal and cancer stem cells, with special reference to the central nervous system. Curr Med Chem. 2009; 16:854–66. [PubMed: 19275598]
50. Bjerkvig R, Johansson M, Miletic H, Niclou SP. Cancer stem cells and angiogenesis. Semin Cancer Biol. 2009; 19:279–84. [PubMed: 19818406]
51. Bourguignon LY, Earle C, Wong G, Spevak CC, Krueger K. Stem cell marker (Nanog) and Stat-3 signaling promote MicroRNA-21 expression and chemoresistance in hyaluronan/CD44-activated head and neck squamous cell carcinoma cells. Oncogene. 2012; 31:149–60. [PubMed: 21685938]
52. Yu CR, Wang L, Khaletskiy A, Farrar WL, Larner A, Colburn NH, et al. STAT3 activation is required for interleukin-6 induced transformation in tumor-promotion sensitive mouse skin epithelial cells. Oncogene. 2002; 21:3949–60. [PubMed: 12037677]

Translational relevance

Despite a trend toward overall improvement in early detection and therapy outcomes, breast cancer (BC) mortality remains unacceptably high due to the ineffectiveness of the control over the recurrent and metastatic lesions, especially for HER2-negative BC. Herein, we identified a population of breast cancer stem cells (BCSCs) expressing HER2 ($HER2^{+}/CD44^{+}/CD24^{-/low}$) isolated from radiation-resistant HER2-negative breast cancer cells and the $HER2^{+}/CD44^{+}/CD24^{-/low}$ was more frequently detected in the recurrent tumors compared with the primary breast cancer. A HER2-linked protein network, such as HER2-STAT3, was detected in the HER2-postive BCSCs by proteomics analysis. Thus the HER2-associated signaling network may be an effective target to treat resistant breast tumors with $HER2^{-/low}$ status.

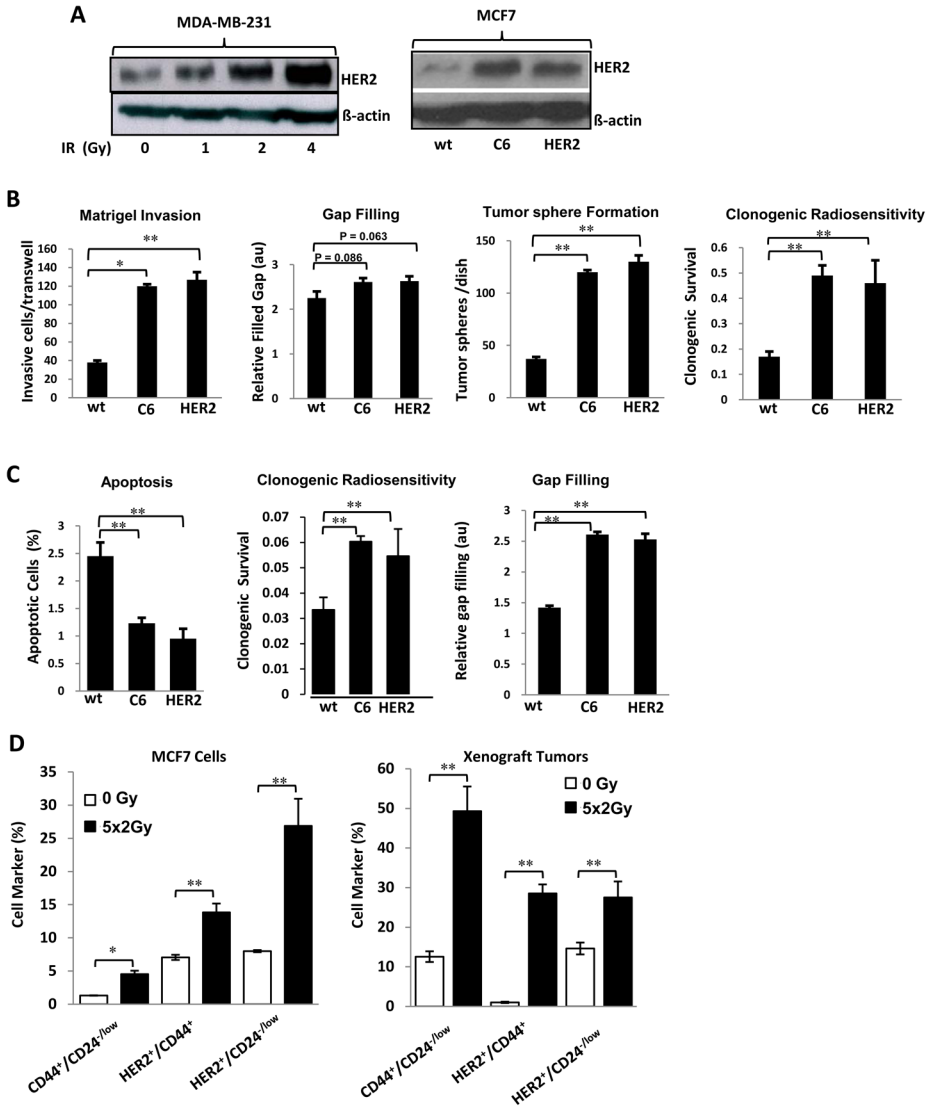

Figure 1.

HER2 protein expression causes the aggressive growth in breast cancer cells with $HER2^{-/low}$ status. **(A)** HER2 protein expression was dose-dependently induced by IR in MDA-MB- 231 cells and in a radioresistant MCF7/C6 (C6) cells (8, 20). MDA-MB-231 were exposed to increased doses of irradiation (0–4 Gy). Twenty-four hours post-irradiation, cells were collected and tested for the expression of HER2. For MCF7/C6 cells, parental MCF7 cells (wt) and MCF7 cells stably transfected with HER2 gene (HER2) were used as negative and positive controls, respectively. **(B)** Evaluation of cell aggressiveness. Matrigel invasion assay: Cells were cultured in Matrigel and cells migrating through the transwell were counted to reflect cell's aggressiveness (mean+SE; n=6; *p<0.05, **p<0.01; Depicted images of invaded cells are illustrated in Fig. S1C). The gap-filling capacity was calculated as the ratio of filled gaps at 96 h post scraping compared to the filled gap at 0 h (Additional data are shown in Fig. S1A). The tumor sphere formation was evaluated as the number of tumor spheres formed per dish (mean+SE; n = 6; **p<0.01; Images of tumor sphere formation are illustrated in Fig. S1D). Clonogenic survival was evaluated as the percentage of cells seeded that were able to form colonies 14 days after irradiation (mean+SE; n = 3; **p<0.01). **(C)** The radioresistant phenotype of MCF7/C6 (C6) cells was compared with

MCF7/HER2 (HER2) and the parental MCF7 cells after treatment with 5 Gy IR by measuring apoptosis, clonogenic survival, and gap filling rates (mean+SE; n=3; **p<0.01). **(D)** Quantification of BCSCs with the feature of $HER2^{+}/CD44^{+}/CD24^{-/low}$ in the surviving fraction of MCF7 cells (left) or xenograft tumors (right) treated with 5 × 2 Gy IR. Cell suspensions from control (sham) or irradiated cells or tumors were sorted by FACS with conjugated antibodies (APC for HER2, PE for CD44, and FITC for CD24; n = 3 from separate sorting, *p<0.05, **p<0.01; additional FACS data are shown in Fig. S3 and Table S1).

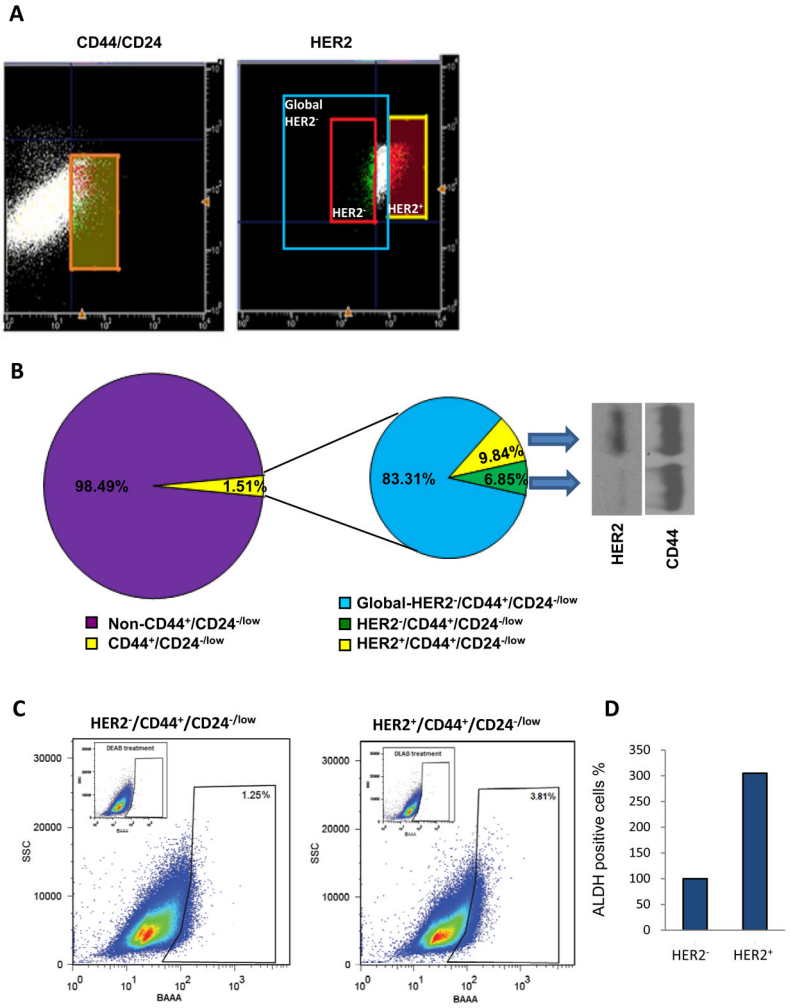

Figure 2.

Characterization of the HER2^{+}/CD44^{+}/CD24$^{-/low}$ BCSCs within MCF7/C6 cell lines. **(A)** CD44^{+}/CD24$^{-/low}$ cells were sorted from 2.5 × 10^{7} MCF/C6 cells with CD44 and CD24 antibodies (left panel), from which the cells were further sorted with HER2 antibody (right panel). The orange box in the left panel indicates the CD44^{+}/CD24$^{-/low}$ fraction used for sorting HER2^{+}/CD44^{+}/CD24$^{-/low}$ (yellow box), HER2^{-}/CD44^{+}/CD24$^{-/low}$ cells (red box) and a global HER2^{-}/CD44^{+}/CD24$^{-/low}$ population (blue box with a broader gate). **(B)** Percentages of CD44^{+}/CD24$^{-/low}$ and HER2^{+}/CD44^{+}/CD24$^{-/low}$ cells derived from MCF7/C6 cells (left panel, also shown in Table S2). Western blot analysis of HER2 and CD44 protein expression in sorted HER2^{+}/CD44^{+}/CD24$^{-/low}$ and HER2^{-}/CD44^{+}/CD24$^{-/low}$ cells (right panel). **(C)** Analysis of ALDH activity in HER2^{-}/CD44^{+}/CD24$^{-/low}$ versus HER2^{+}/CD44^{+}/CD24$^{-/low}$ cells via flow cytometry using Aldefluor staining. As negative control, cells were incubated with ALDH inhibitor DEAB. **(D)** Quantification of the ALDH expression HER2^{+}/CD44^{+}/CD24$^{-/low}$ compared to HER2^{-}/CD44^{+}/CD24$^{-/low}$ BCSCs analysis in C.

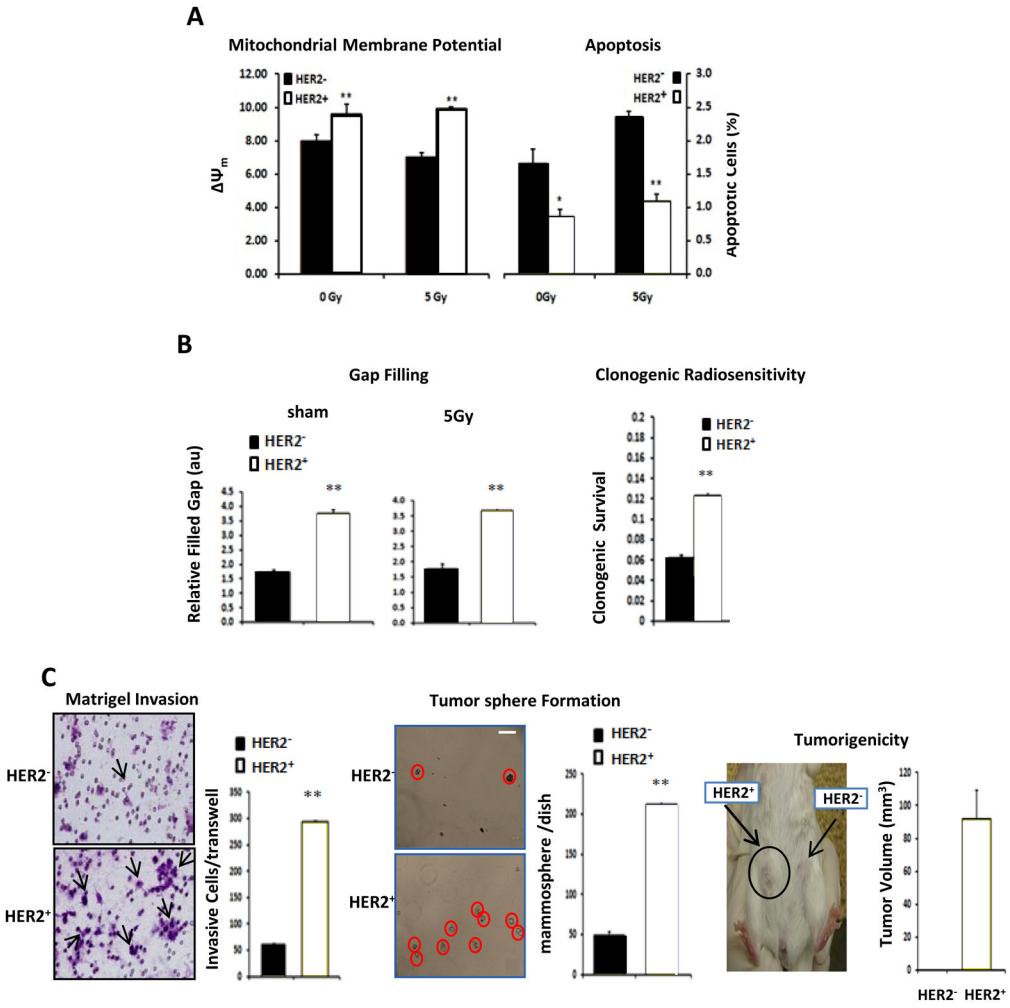

Figure 3.

Enhanced radiation resistance and aggressiveness in HER2^{+}/CD44^{+}/CD24$^{-/low}$ BCSCs. **(A)** Mitochondrial membrane potential (left panel) and apoptosis (right panel) were measured in HER2^{+}/CD44^{+}/CD24$^{-/low}$ and HER2^{-}/CD44^{+}/CD24$^{-/Low}$ BCSCs treated with or without 5 Gy IR for 24 h. Data represents mean+ SE of 3 independent experiments and statistical significance was evaluated as *p<0.05; **p<0.01. **(B)** Enhanced radioresistance in HER2^{+}/CD44^{+}/CD24$^{-/low}$ cells treated with sham (0 Gy) or 5 Gy of IR is tested by gap filling and clonogenic survival assays. The gap-filling rate (left panel) was calculated as the ratio of the filled gap at 96 h compared with 0 h. The clonogenic survival (right panel) of HER2^{+}/CD44^{+}/CD24$^{-/Low}$ BCSCs was evaluated by counting the number of colony formation (more than 50 cells) 14th day after cells were treated with 5 Gy of IR (n = 6 and **p<0.01; Additional data are shown in Fig. S5). **(C)** The aggressiveness of HER2^{-}/CD44^{+}/CD24$^{-/low}$ (HER2^{-}) and HER2^{+}/CD44^{+}/CD24$^{-/low}$ (HER2^{+}) BCSCs was further analyzed by Matrigel invasion assay (left panel), tumor sphere formation (middle panel, n = 6; **p<0.01; scale bar = 50 μm) and *in vivo* tumorigenesis (right panel). Tumor numbers and volumes were measured in NOD/SCID mice two weeks after the inoculation of 500 cells from each BCSC population in two opposite site (HER+ left side and HER- right side) of the animal as depicted by arrows.

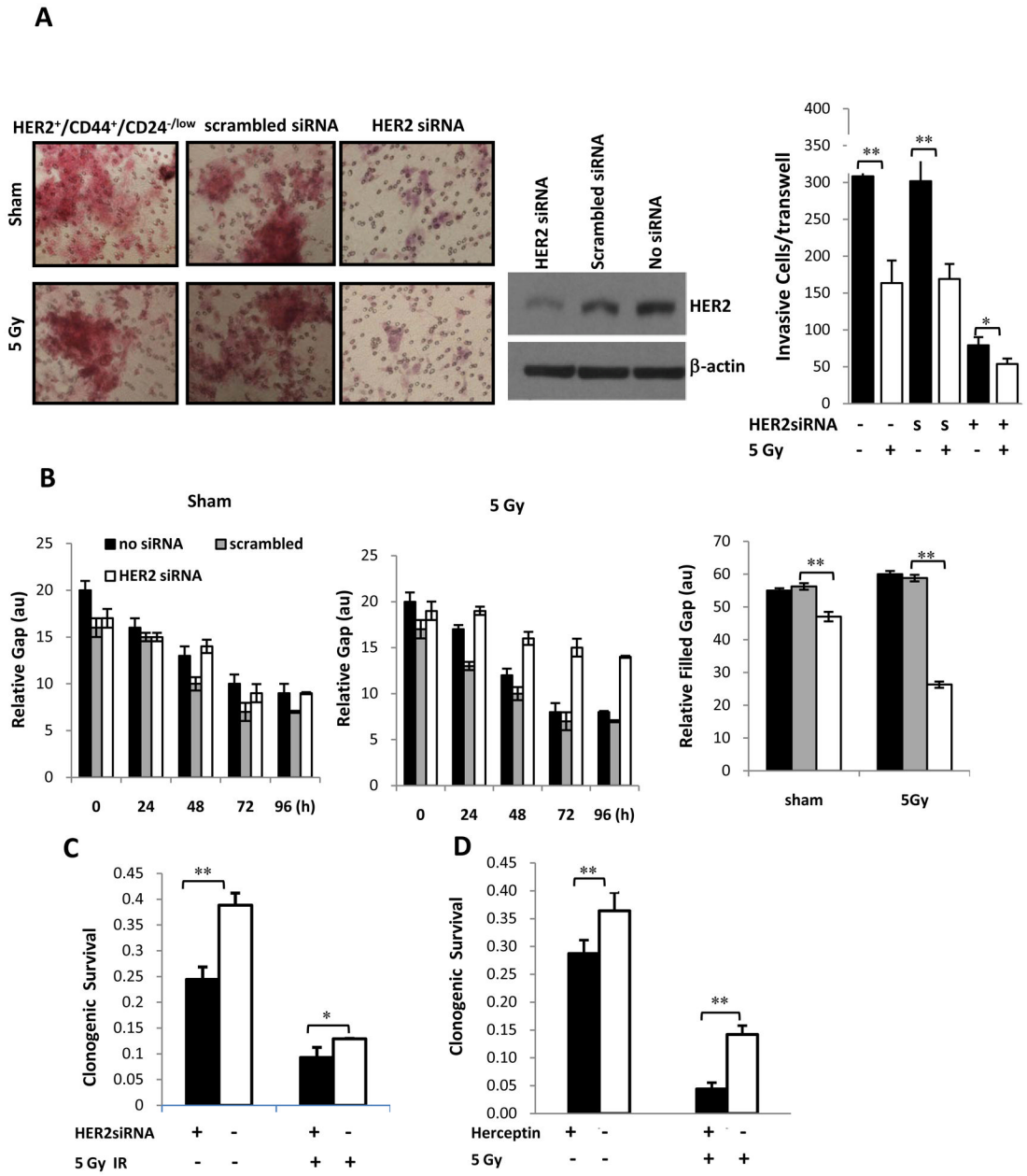

Figure 4.

Inhibition of HER2 blocks the aggressiveness and radioresistant phenotypes of $HER2^{+}/CD44^{+}/CD24^{-/low}$ BCSCs. **(A)** Left panel represents depicted images of Matrigel invasion assays of $HER2^{+}/CD44^{+}/CD24^{-/low}$ BCSCs at 72 h after 5 Gy IR and treatment with scrambled or specific HER2 siRNA. Middle panel, depicts the specific capacity of HER2 siRNA to reduce HER2 expression in $HER2^{+}$ breast cancer stem cells. Right panel represents quantification of the number of cells invading the membrane per transwell. Data represents mean+SE of n = 6 and statistical analysis was performed with *p<0.05, **p<0.01). **(B)** Represents the gap filling values determined at different time points post cell's injury (0 to 96 h) in sham (0 Gy) and irradiated cells (5Gy) and in cells treated with specific or scrambled siRNA against HER2. Right panel represent mean +SE of the gap filling rate calculated from n = 6 independent experiments; **p<0.01). **(C, D)** The effect of

targeting HER2 signaling pathway on aggressiveness and radiosensitivity of BCSCs. $HER2^{+}/CD44^{+}/CD24^{-/low}$ were treated either with siRNA (C; n = 3; *p<0.05; **p<0.01) or with anti- HER2 antibody, Herceptin, (D; 10 μg/ml for 5 days, n = 3; **p<0.01). The clonogenic sensitivity to IR was evaluated following sham or 5 Gy IR (mean+SE; n=3).

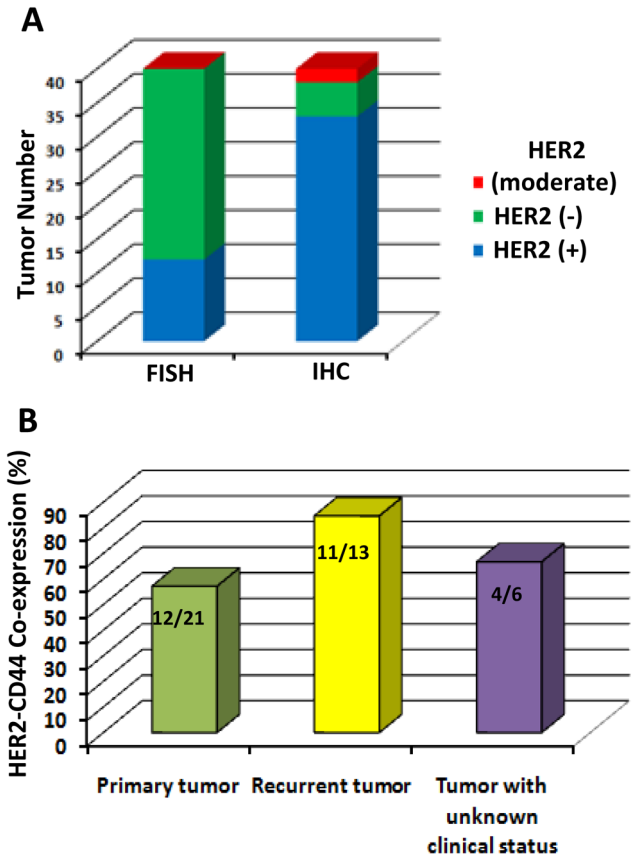

Figure 5.

Increased number of HER2$^+$/CD44$^+$ cells in recurrent breast cancer. **(A)** HER2 expression status was assessed in breast cancer samples that were diagnosed as primary, recurrent or unknown status by FISH and IHC. Blue: HER2 + (IHC 2+ and 3+) or amplified (FISH, HER2: centromere 17 signal ratio >2.2); Green: HER2-(IHC 0) or non-amplified (FISH, HER2:centromere 17 signal ratio <1.8); Red: HER2 equivocal (IHC 1+ and FISH, HER2:centromere 17 signal ratio =1.8 – 2.2). **(B)** Data of immunohistochemistry analysis for the expression of HER2 and CD44 in tumors harvested from breast cancer patients. Positive cells are depicted with arrows. HER2$^-$/CD44$^-$ tumor was assigned if no HER2$^+$/CD44$^+$ cells were detected. Positive tumors were assigned if at least one cluster of HER2$^+$/CD44$^+$ was detected (Additional staining results are shown in Fig. S6).

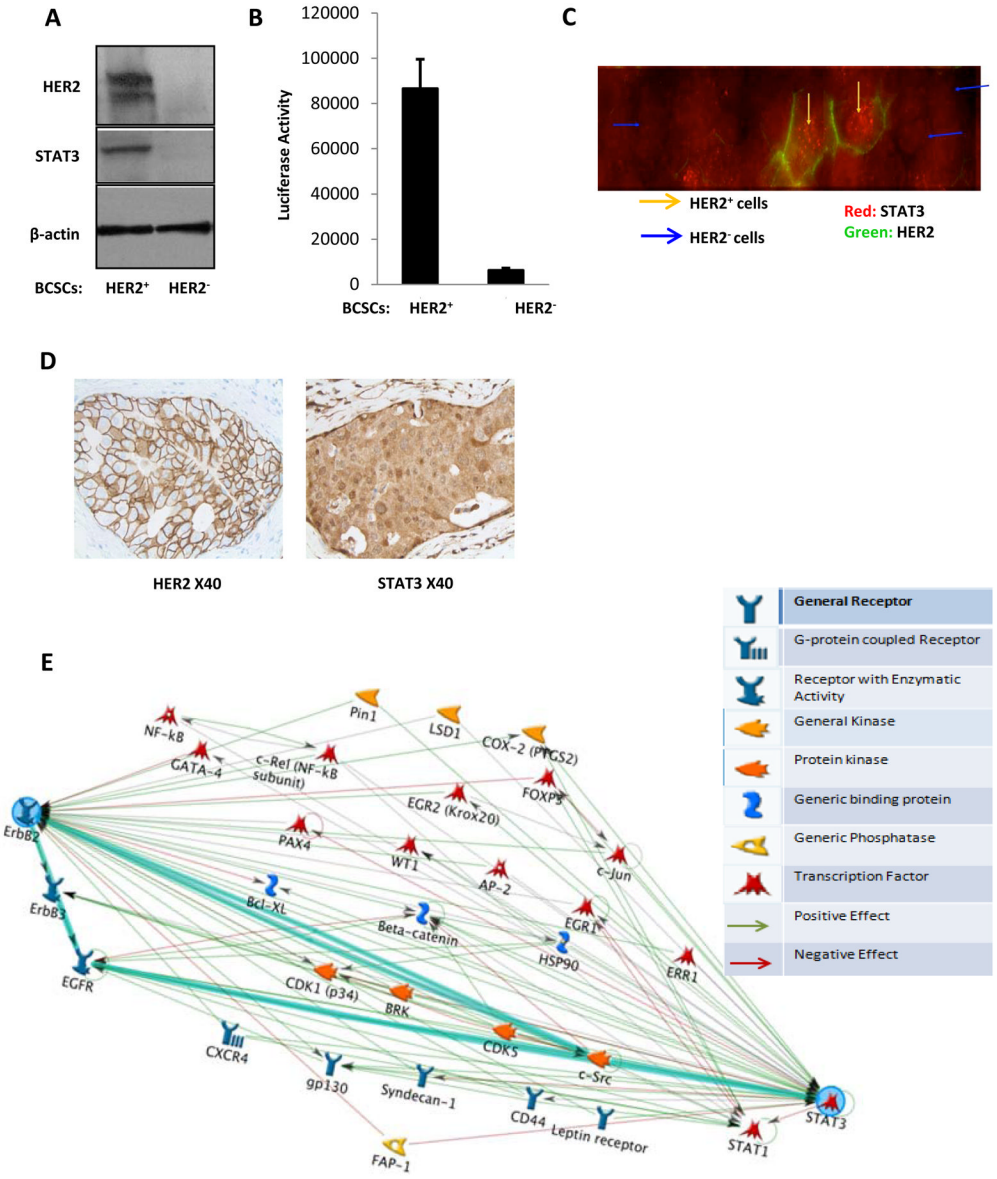

Figure 6.

HER2 and STAT3 crosstalk in HER2^{+}/CD44^{+}/CD24$^{-/low}$ BCSCs. **(A)** HER2 and STAT3 protein expression levels were further determined by Western blot in the HER2^{+}/CD44^{+}/CD24$^{-/low}$ and HER2^{-}/CD44^{+}/CD24$^{-/low}$ BCSCs. **(B)** Increased STAT3 transcriptional activity in HER2^{+}/CD44^{+}/CD24$^{-/low}$ compared to HER2^{-}/CD44^{+}/CD24$^{-/low}$ BCSCs. STAT3 luciferase reporters (52) were transfected in HER2^{+}/CD44^{+}/CD24$^{-/low}$ and HER2^{-}/CD44^{+}/CD24$^{-/low}$ cells and luciferase activity was measured 24 h after transfection (n = 3; **p < 0.01). **(C)** Co-localization of HER2 and STAT3 expression in radio-resistant cancer cells and **(D)** HER2^{+} human breast specimen. **(E)** A putative HER2-STAT3 crosstalk signaling networks for the aggressiveness of HER2^{+}/CD44^{+}/CD24$^{-/low}$ BCSCs. For the interaction between HER2 and STAT3 signals, a cluster of factors searched from the database of MetaCore™ Version 6.9, was identified to interact with both STAT3 and HER2. This network causing a crosstalk between HER2 and STAT3 may play a critical role for the

overall aggressiveness of the HER2 expressing breast cancer stem cells in breast tumors with $HER2^{-/low}$ status.